

Electronic Supplementary Information

Luminescent Dicyanidonitridotechnetium(V) Core with a Tridentate Ligand Coordination Sites

Takashi Yoshimura,^{*a,b} Kojiro Nagata,^a Tatsuki Shiroyama,^c Yasushi Kino,^d Tsutomu Takayama,^e Tsutomu Sekine^f and Atsushi Shinohara^{b,c}

^aRadioisotope Research Center, Institute for Radiation Sciences, Osaka University, Suita, Osaka 565-0871, Japan,

^bProject Research Center for Fundamental Sciences, Graduate School of Science, Osaka University, Toyonaka, Osaka 560-0043, Japan, ^cDepartment of Chemistry, Graduate School of Science, Osaka University, Toyonaka, Osaka 560-0043, Japan, ^dDepartment of Chemistry, Graduate School of Science, Tohoku University, Sendai, Miyagi 980-8576, Japan,

^eDepartment of Chemistry, Daido University, Nagoya, Aichi 457-8530, Japan, ^fInstitute for Excellence in Higher Education, Tohoku University, Sendai, Miyagi 980-8576, Japan.

Experimental Section

Materials. All commercially available reagents were used as received. The isotope ⁹⁹Tc was used to synthesize all of the Tc complexes reported in this paper. *Caution:* ⁹⁹Tc is a low-energy β^- emitter ($E_{\max} = 290$ keV) with a half-life of 2.11×10^5 y. $n\text{-}(C_4H_9)_4N[TcNCl_4]$ was prepared according to literature procedures.¹

Synthesis of the Complexes.

[TcNCl₂bpa] (1). $(n\text{-}C_4H_9)_4N[^{99}\text{TcNCl}_4]$ (6.1 mg, 1.2×10^{-2} mmol) was dissolved in 0.5 mL of CH₃CN, and 0.65 μ L of CH₃CN solution containing bpa (7.2 mg, 3.6×10^{-2} mmol) was added to the solution. The mixture was sonicated for several minutes, and then the solution was left for several hours. The brown crystals deposited were collected by filtration. Yield: 4.4 mg (89%). UV-vis/cm⁻¹ ($\varepsilon/M^{-1}cm^{-1}$) in CH₃CN: 21200 (800), 26600 (5300), 39400 (8000).

[TcN(CN)₂bpa] (2). The complex 1 (2.0 mg, 4.9×10^{-3} mmol) was dissolved in 20 mL of CH₃CN, and 3.5 mL of an aqueous solution containing KCN (0.65 mg, 1.0×10^{-2} mmol) was added to the solution. The mixture was sonicated for 5 min and left for several hours. The solution was evaporated to dryness, and then the residue was dissolved in 10 mL of CH₃CN. Toluene was layered on the solution, and the solution was left for several days. The yellow crystals deposited were collected by filtration. Yield: 0.89 mg (44%). UV-vis/cm⁻¹ ($\varepsilon/M^{-1}cm^{-1}$) in CH₃CN: 22800 (320), 30200 (4600), 37200 (2800), 39800 (9300).

X-ray Crystallography. Single crystal X-ray data were collected at -103 °C on a Rigaku RAXIS diffractometer with graphite-monochromated Mo $K\alpha$ radiation. Cell parameters were retrieved using CrystalClear Software. Diffraction data were collected and processed using CrystalClear. Crystal structures were solved by SHELXT version 2014.² Atomic coordinates and thermal parameters of non-hydrogen atoms were calculated by a full-matrix least-squares method

(SHELXL version 2017).³ Calculations were performed using Crystal Structure 4.2.4.⁴ A large residual electron density for **2** results from the limited data quality.

Physical Measurements. UV-vis spectra were measured by a JASCO V-550 spectrophotometer. IR spectra were recorded in KBr pellets on a JASCO FTIR-6100 spectrometer. For measurement of emission spectrum, a solid sample was placed between two nonfluorescent glass plates. The corrected emission spectrum was recorded on a multichannel photodetector (Hamamatsu Photonics, PMA-11) at 365 nm (± 5 nm) excitation by using a 100 W mercury-xenon lamp (HOYA-SCHOTT HLS 100UM) and an optical band-pass filter (Asahi Spectra).

DFT Calculations. DFT calculations were performed with the Amsterdam Density Functional package (ADF 2017.103).^{5,6} For geometry optimizations and calculation of frequencies, the initial geometries of [TcNCl₂(bpa)] and [TcN(CN)₂(bpa)] were taken from the X-ray structures. Structural optimizations were carried out at the GGA level using PBE, the scalar relativistic ZORA, and the DZ for all atoms with a small frozen core approximation as provided in the ADF basis set library.⁷ Calculation of all positive IR frequencies confirmed the existence of the potential minimum. The atomic coordinates of the optimized geometries are listed in Tables S2 – S4. The single point and time dependent DFT calculations of **1** and **2** were performed using the optimized geometries at B3LYP, the scalar relativistic ZORA, and the TZ2P as provided in the ADF basis set library. The calculations for **1** and **2** used the COSMO solvent model for CH₃CN.⁸ In the case of **2***, the single point energy calculations was performed using the GGA level using PBE, the scalar relativistic ZORA, and the DZ for all atoms with a small frozen core approximation as provided in the ADF basis set library.

References

- 1 J. Baldas, J. F. Boas, J. Bonnyman and G. A. Williams, *J. Chem. Soc., Dalton Trans.*, 1984, 2395-2400.
- 2 G. M. Sheldrick, *Acta Cryst. A*, 2015, **A71**, 3-8.
- 3 G. M. Sheldrick, *Acta Cryst. C*, 2015, **C71**, 3-8.
- 4 Rigaku Corporation, Tokyo, Japan.
- 5 G. te Velde, F. M. Bickelhaupt, E. J. Baerends, C. Fonseca Guerra, S. J. A. van Gisbergen, J. G. Snijders, and T. Ziegler , *J. Comput. Chem.* 2001, **22**, 931-967.
- 6 ADF2017, S., Theoretical Chemistry; Vrije Universiteit; Amsterdam, T. N., <http://www.scm.com/>.
- 7 E. van Lenthe, A. Ehlers, E.-J. Baerends, *J. Chem. Phys.* 1999, **110**, 8943-8953.
- 8 C. C. Pye, T. Ziegler, *Theo. Chem. Acc.* 1999, **101**, 396-408.

Table S1. Crystallographic data of [TcNCl₂(bpa)] (**1**) and [TcN(CN)₂(bpa)] (**2**)

	1	2
Formula	C ₁₄ H ₁₆ Cl ₂ N ₅ Tc	C _{17.5} H ₁₇ N ₆ Tc
F.W.	424.13	410.28
Space group	P2 ₁ /c	P $\bar{1}$
<i>a</i> /Å	10.2820(3)	7.3182(3)
<i>b</i> /Å	11.9687(3)	10.7602(4)
<i>c</i> /Å	14.2478(5)	12.5043(5)
α /deg		66.5421(17)
β /deg	103.6947(8)	87.0938(14)
γ /deg		72.793(2)
<i>V</i> /Å ³	1703.52(9)	860.32(6)
<i>Z</i>	4	2
<i>T</i> /K	170.0	170.0
ρ_{calc} /gcm ⁻³	1.646	1.576
μ /mm ⁻¹	1.153	0.840
<i>R</i> 1	0.0469	0.0795
<i>wR</i> 2	0.0958	0.2022
GOF	1.164	1.209

Table S2. Atomic Coordinates of Optimized Geometry for **1**

	x/ \AA	y/ \AA	z/ \AA
Tc1	1.48575857	2.28461741	1.26347497
Cl1	-0.90084901	2.20389450	1.20151557
Cl2	1.52215185	-0.03237840	1.83812249
N1	1.42166253	4.01704463	0.00878243
N2	1.89602734	3.11785124	2.62947182
N3	3.49095431	2.10526204	0.54630770
N4	1.29743724	1.44519778	-1.00120630
C1	4.53898505	2.63979204	1.22539462
C2	5.82135300	2.68834793	0.70724388
C3	6.06663787	2.17540330	-0.56626227
C4	5.00008400	1.61484231	-1.26064154
C5	3.73411351	1.57481580	-0.68468718
C6	2.59067541	0.86260632	-1.35695450
C7	1.69933060	5.25599551	0.49166682
C8	1.82738427	6.36667304	-0.32400808
C9	1.67685404	6.22633445	-1.70338493
C10	1.37986265	4.96269641	-2.20212002
C11	1.23968471	3.88388033	-1.33463055
C12	0.78548953	2.53597849	-1.82947795
H1	4.30248193	3.03605040	2.21217823
H2	6.61853952	3.13025823	1.30599848
H3	7.06446284	2.20835118	-1.00564714
H4	5.14174224	1.18875223	-2.25538358
H5	2.58573611	-0.17273455	-0.97393407
H6	2.75616373	0.82730024	-2.44999894
H7	1.81956660	5.32006607	1.57248006
H8	2.04930171	7.33410510	0.12794655
H9	1.78471235	7.08114633	-2.37234188
H10	1.23914062	4.80180072	-3.27236691
H11	1.04390320	2.41722988	-2.89827992
H12	-0.31407003	2.51399678	-1.73520745
H13	0.58734334	0.71609813	-0.87086382

Table S3. Atomic Coordinates of Optimized Geometry for **2**

	x/ \AA	y/ \AA	z/ \AA
Tc1	-0.84162330	0.84565462	0.08381351
N1	-2.03681542	0.09163148	0.94362684
N2	-1.66473413	3.94141337	-0.27725513
N3	-1.40172099	0.27539680	-3.03998288
N4	0.62371452	-0.76094671	-0.00066881
N5	0.43685670	1.55755684	1.69078158
N6	1.14118064	1.78053070	-0.98749217
C1	-1.51394077	2.78362621	-0.14653223
C2	-1.33769699	0.47029502	-1.88340061
C3	0.43832795	-1.91604769	0.68387438
C4	1.42766913	-2.87697944	0.81023206
C5	2.67128982	-2.65510856	0.22153586
C6	2.86040552	-1.47983179	-0.49624106
C7	1.82230617	-0.55834007	-0.60671612
C8	1.94284238	0.65889876	-1.48458729
C9	0.18090629	1.24500161	2.98440625
C10	1.06032195	1.54198626	4.01236552
C11	2.26466135	2.17769913	3.71495910
C12	2.52447619	2.51277957	2.39112260
C13	1.59320802	2.20839711	1.40143816
C14	1.77442130	2.67898227	-0.01813076
H1	-0.54534377	-2.04369155	1.13502177
H2	1.21763283	-3.78829952	1.37187118
H3	3.47593736	-3.38618401	0.31570579
H4	3.81201829	-1.27068305	-0.98803885
H5	3.00728367	0.92582392	-1.62126228
H6	1.52648940	0.38440022	-2.47045913
H7	-0.76839917	0.74312451	3.16942238
H8	0.79720062	1.27006556	5.03556268
H9	2.98400373	2.41290780	4.50097736
H10	3.44632676	3.02708465	2.11413072
H11	1.25203017	3.64962117	-0.09850885
H12	2.84690668	2.84576972	-0.23034035
H13	0.75995218	2.31908385	-1.77462013

Table S4. Atomic Coordinates of Optimized Geometry for **2***

	x/ \AA	y/ \AA	z/ \AA
Tc1	-0.94375128	0.95713343	-0.04361590
N1	-1.91626419	0.03527485	0.97641188
N2	-1.79154466	4.06250083	0.08429151
N3	-1.50004252	0.21964623	-3.13200854
N4	0.62320781	-0.88754753	-0.09204960
N5	0.54079025	1.36728232	1.63558051
N6	1.13486960	1.71302112	-1.03661170
C1	-1.53894373	2.91305119	0.02779449
C2	-1.38959730	0.47018684	-1.98691905
C3	0.47730131	-1.93226550	0.73936734
C4	1.54560911	-2.73254354	1.12448845
C5	2.82083287	-2.42414467	0.65079972
C6	2.97324216	-1.33441762	-0.20563910
C7	1.85240949	-0.59398115	-0.56840262
C8	1.91445250	0.56021069	-1.53308360
C9	0.29489540	1.00961014	2.91458347
C10	1.15464032	1.33079855	3.95249960
C11	2.32079957	2.04194780	3.66776729
C12	2.57236709	2.41134611	2.34806301
C13	1.66014991	2.07165679	1.35443668
C14	1.81854457	2.56874910	-0.06092574
H1	-0.54191346	-2.10519575	1.09591167
H2	1.37728336	-3.58378795	1.78602154
H3	3.68583004	-3.01898316	0.94882388
H4	3.95470276	-1.06448860	-0.59968747
H5	2.96551241	0.83191265	-1.74098913
H6	1.44109663	0.24366210	-2.47857723
H7	-0.63074800	0.45143667	3.07211680
H8	0.91251148	1.01954856	4.96965932
H9	3.02073357	2.30865373	4.46124871
H10	3.47058319	2.97269275	2.08477112
H11	1.33220028	3.56065644	-0.10468056
H12	2.89136576	2.70129953	-0.29603964
H13	0.82888530	2.28119352	-1.83693560

Table S5. Selected Observed and Calculated Bond Distances (\AA) and Angles (deg) of **1**, **2**, and **2***

	1		2		2*
	Observed	Calcd	Observed	Calcd	Calcd
Tc≡N	1.646(3)	1.652	1.645(7)	1.654	1.684
Tc–X	2.3990(9), 2.4032(9)	2.388, 2.389	2.070(7), 2.093(7)	2.063, 2.064	2.046, 2.052
Tc–N(eq)	2.135(3), 2.138(3)	2.137, 2.140,	2.166(5), 2.196(5)	2.173, 2.176	2.279, 2.421
Tc–N(ax)	2.382(3)	2.4226	2.378(5)	2.440	2.424
N≡Tc–N(eq)	94.96(13)	94.8, 95.0	95.9(3), 98.2(3)	99.8, 101.0	88.2, 91.6
N≡Tc–N(ax)	165.70(12)	165.3	164.5(3)	171.9	156.0
N≡Tc–X	102.16(11), 103.65(11)	106.7	98.7(3), 99.6(3)	103.8, 104.5	108.6, 109.5
X–Tc–X	89.05(3)	89.4	87.2(2)	89.2	101.3
X–Tc–N(eq)	89.18(8), 90.52(8)	89.0, 89.1	87.8(2), 89.8(2)	88.1, 89.5	86.6, 89.5
X–Tc–N(ax)	161.26(8), 162.48(8)	157.8, 158.0	162.9(2), 164.5(3)	155.0, 155.3	151.9, 156.6
X–Tc–N(ax)	86.60(7), 87.77(7)	83.5, 83.7	90.3(2), 93.4(2)	81.2, 81.7	82.7, 88.0
N(eq)–Tc–N(eq)	85.62(11)	84.2	90.67(19)	82.8	74.4
N(eq)–Tc–N(ax)	74.69(11), 74.72(10)	74.3, 74.3	71.4(2), 73.67(19)	73.7, 73.8	71.0, 71.8

X = Cl for **1** and X = C for **2**.

Table S6. Selected Observed and Calculated IR Frequencies of **1**

wavenumber/cm ⁻¹		
Observed	Calcd	Assignment
2924	2923	ν C-H(methylene)
1608	1587	ν phenyl
1482	1456	ν phenyl
1433	1417	ν phenyl
	1411	δ methylene
1287	1266, 1260	δ phenyl
1159	1147	δ phenyl
1102	1114	ν C-N
1058	1086	ν N≡Tc
772	765	γ phenyl

Table S7. Selected Observed and Calculated IR Frequencies of **2**

Wavenumber/cm ⁻¹		
Observed	Calcd	Assignment
2922	2923	ν C-H(methylene)
2123, 2112	2134, 2127	ν C≡N
1608	1590	ν phenyl
1449	1457	ν phenyl
	1418	δ methylene
1294	1264	δ phenyl
1157	1151	δ phenyl
1094	1106	ν C-N
1055	1089	ν N≡Tc
773	740	γ phenyl

Table S8. Observed and Calculated Electronic Transition Energies of **1**

Wavenumber/cm ⁻¹			
Observed	Calcd	Oscillator Strength	Major component of transition
21200 sh	24096	0.0001	$d_{xy} \rightarrow d_{\pi^*}$ [HOMO → LUMO+2 (71.1%), HOMO → LUMO+1 (28.7%)]
	24849	0.0040	$d_{xy} \rightarrow d_{\pi^*}$ [HOMO → LUMO+3 (93.6%), HOMO → LUMO (6.1%)]
26600	26294	0.0937	$d_{xy} \rightarrow \pi^*(bpa)$ [HOMO → LUMO (92.7%), HOMO → LUMO+3 (6.1%)]
	27006	0.1131	$d_{xy} \rightarrow \pi^*(bpa)$ [HOMO → LUMO+1 (70.4%), HOMO → LUMO+2 (28.4%)]
39400	37739	0.0187	$p(N_{amine})$, $p(Cl)$, $p(N_{nitrido}) \rightarrow d_{\pi^*}$ (63.4%) $p(N_{amine})$, $p(Cl)$, $p(N_{nitrido}) \rightarrow \pi^*(bpa)$ (31.3%)
	39421	0.0112	$p(Cl) \rightarrow \pi^*(bpa)$ (46.8%) $p(N_{amine})$, $p(Cl)$, $p(N_{nitrido}) \rightarrow \pi^*(bpa)$ (26.1%) $\pi(bpa) \rightarrow \pi^*(bpa)$ (17.2%)
	40503	0.0151	$p(Cl) \rightarrow d_{\pi^*}$ (77.0%)
	42243	0.0230	$p(Cl) \rightarrow d_{\pi^*}$ (35.2%) $p(Cl) \rightarrow \pi^*(bpa)$ (16.8%) $\pi(bpa) \rightarrow \pi^*(bpa)$ (15.2%) $p(N_{amine})$, $p(Cl)$, $p(N_{nitrido}) \rightarrow \pi^*(bpa)$ (14.1%)
	43109	0.0296	$p(Cl)$, $p(N_{nitrido}) \rightarrow \pi^*(bpa)$ (35.8%) $p(Cl) \rightarrow \pi^*(bpa)$ (20.2%) $\pi(bpa) \rightarrow \pi^*(bpa)$ (15.4%)
	44146	0.0634	$p(Cl)$, $p(N_{nitrido}) \rightarrow \pi^*(bpa)$ (48.5%) $\pi(bpa) \rightarrow \pi^*(bpa)$ (14.0%)

Table S9. Observed and Calculated Electronic Transition Energies of **2**

Wavenumber/cm ⁻¹			
Observed	Calcd	Oscillator Strength	Major component of transition
22800	26541	0.0063	$d_{xy} \rightarrow d_{\pi^*}$ [HOMO \rightarrow LUMO (51.6%), HOMO \rightarrow LUMO+1 (37.1%), HOMO \rightarrow LUMO+2 (11.0%)]
	26735	0.0059	$d_{xy} \rightarrow d_{\pi^*}$ [HOMO \rightarrow LUMO+1 (61.6%), HOMO \rightarrow LUMO (24.7%), HOMO \rightarrow LUMO+2 (13.4%)]
30200	30419	0.1003	$d_{xy} \rightarrow \pi^*(bpa)$, d_{π^*} [HOMO \rightarrow LUMO+2 (74.9%), HOMO \rightarrow LUMO (23.0%)]
	31870	0.0995	$d_{xy} \rightarrow \pi^*(bpa)$ [HOMO \rightarrow LUMO+3 (99.1%)]
37200	36946	0.0199	p(N _{amine}), p(N _{nitrido}) \rightarrow d_{π^*} (83.4%)
	37193	0.0153	p(N _{amine}), p(N _{nitrido}) \rightarrow d_{π^*} (72.8%)
	37245	0.0086	$d_{xy} \rightarrow \pi^*(bpa)$ (74.7%) $\pi(bpa) \rightarrow d_{\pi^*}$ (13.4%)
39800	41992	0.0116	$\pi(bpa) \rightarrow \pi^*(bpa)$ (46.4%) $\pi(bpa) \rightarrow d_{\pi^*}$ (44.3%)
	43842	0.0521	p(N _{amine}), p(N _{nitrido}) \rightarrow $\pi^*(bpa)$ (36.5%) $\pi(bpa) \rightarrow d_{\pi^*}$ (24.6%) $\pi(bpa) \rightarrow \pi^*(bpa)$ (13.1%)
	44413	0.0667	p(N _{amine}), p(N _{nitrido}) \rightarrow $\pi^*(bpa)$ (57.2%) $\pi(bpa) \rightarrow d_{\pi^*}$ (14.4%)

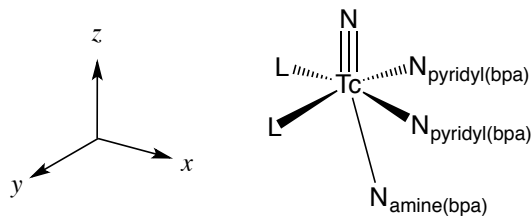


Fig. S1. The axes in the present study ($L = Cl$ or CN).

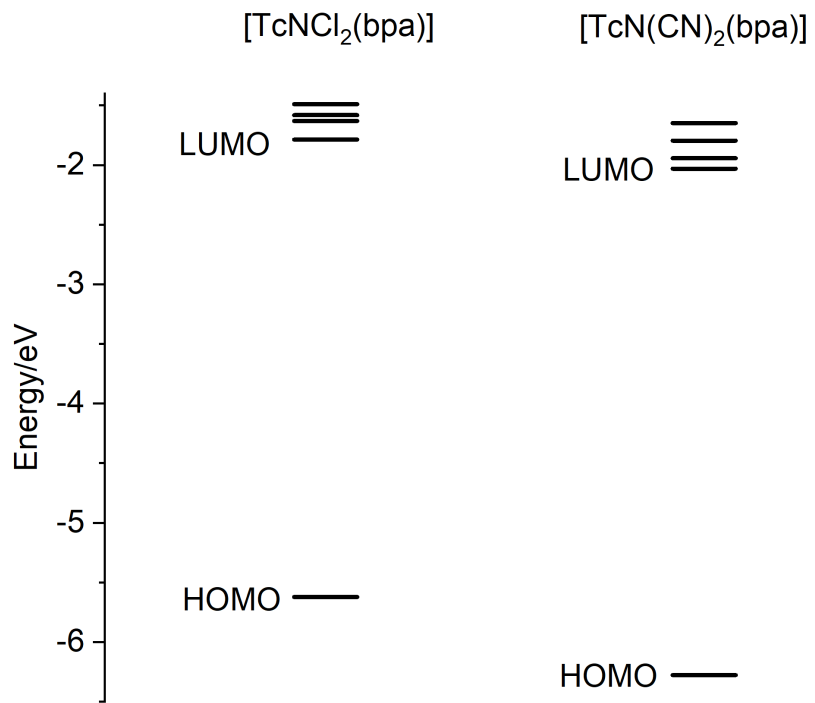
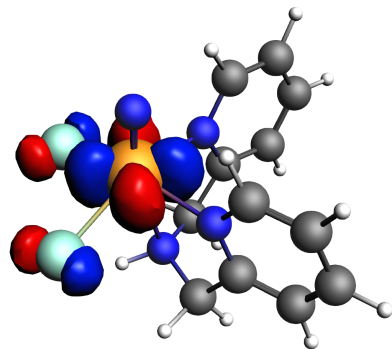
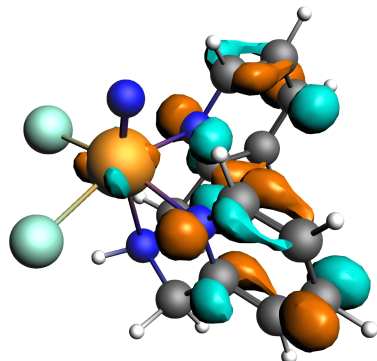


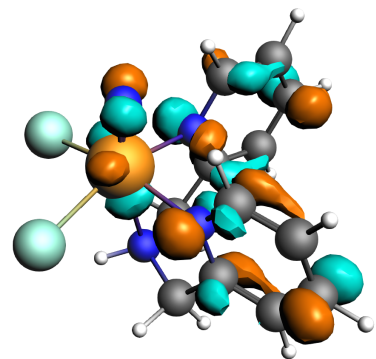
Fig. S2. Energy diagrams in near HOMO/LUMO levels of $[TcNCl_2(bpa)]$ (1) and $[TcN(CN)_2(bpa)]$ (2).



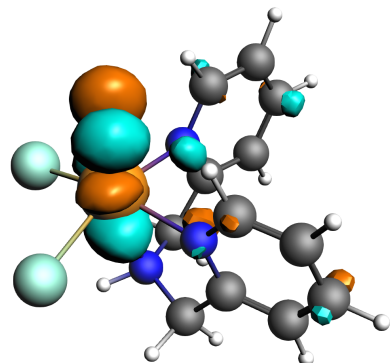
HOMO (-5.62 eV)



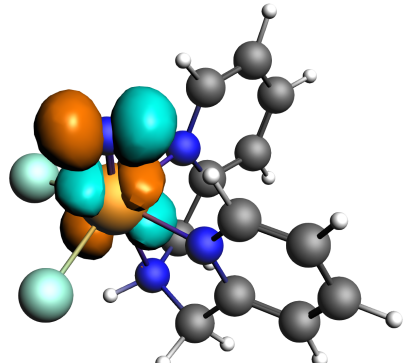
LUMO (-1.79 eV)



LUMO+1 (-1.63 eV)

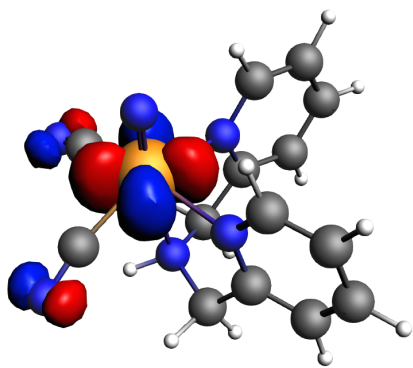


LUMO+2 (-1.58 eV)

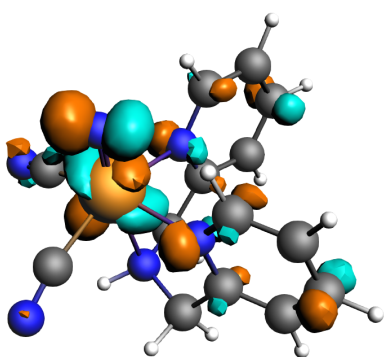


LUMO+3 (-1.49 eV)

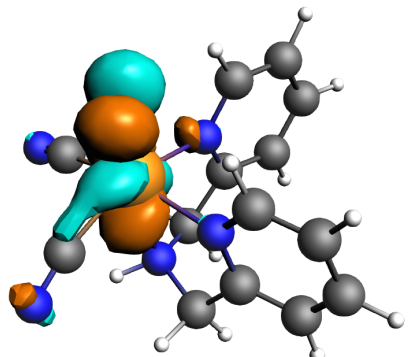
Fig. S3. Contour plots of MOs near the frontier orbital levels of $[TcNCl_2(bpa)]$ (**1**).



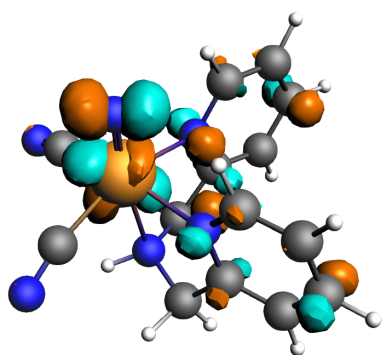
HOMO (-6.28 eV)



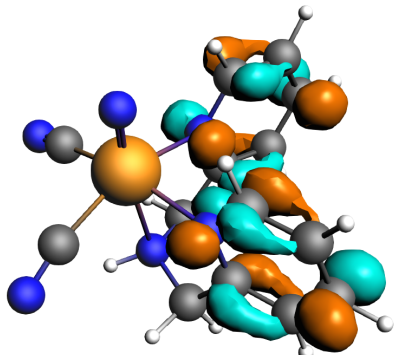
LUMO (-2.03 eV)



LUMO+1 (-1.94 eV)



LUMO+2 (-1.79 eV)



LUMO+3 (-1.65 eV)

Fig. S4. Contour plots of MOs near the frontier orbital levels of $[TcN(CN)_2(bpa)]$ (**2**).

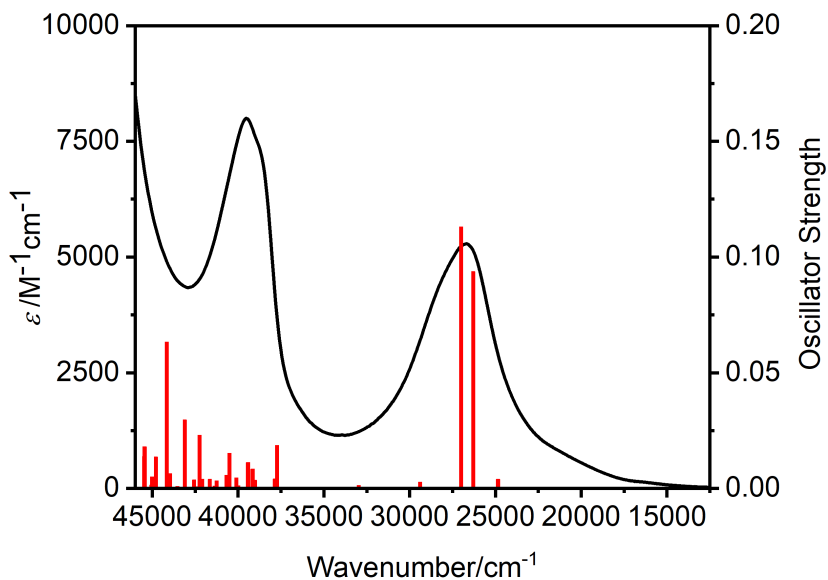


Fig. S5. Observed and calculated UV-vis spectra for **1** in CH_3CN (black: observed and red: calculated spectra).

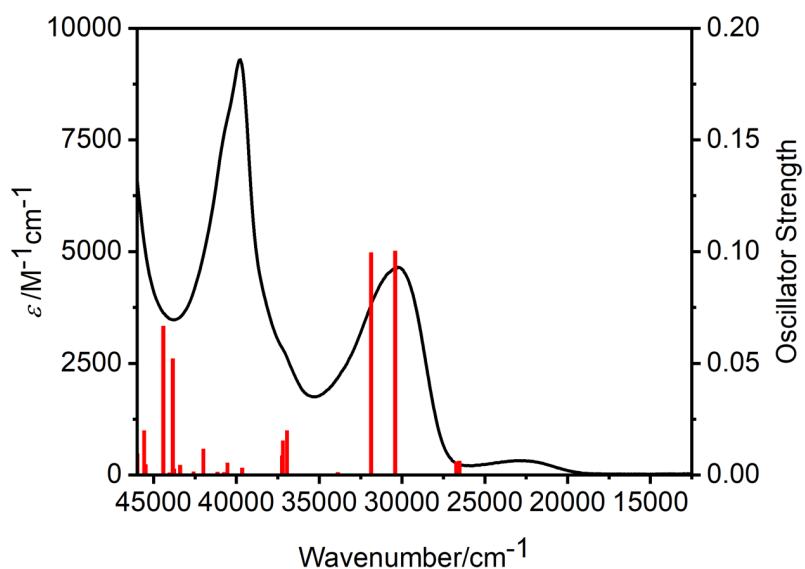


Fig. S6. Observed and calculated UV-vis spectra for **2** in CH_3CN (black: observed and red: calculated spectra).